OPEN

Quantitative Measurement of Intact Alpha-Synuclein Proteoforms from Post-Mortem Control and Parkinson's Disease Brain Tissue by Intact Protein Mass Spectrometry

John F. Kellie[1], Richard E. Higgs[2], John W. Ryder[2], Anthony Major[2], Thomas G. Beach[3], Charles H. Adler[4], Kalpana Merchant[5] & Michael D. Knierman[2]

[1]GSK, 709 Swedeland Road, King of Prussia, PA, [2]Eli Lilly and Company, Lilly Corporate Center, Indianapolis, IN, [3]Civin Laboratory for Neuropathology, Banner Sun Health Research Institute, Sun City, AZ, [4]Department of Neurology, Mayo Clinic Arizona, Scottsdale, AZ, [5]TransThera Consulting Co., Indianapolis, IN.

A robust top down proteomics method is presented for profiling alpha-synuclein species from autopsied human frontal cortex brain tissue from Parkinson's cases and controls. The method was used to test the hypothesis that pathology associated brain tissue will have a different profile of post-translationally modified alpha-synuclein than the control samples. Validation of the sample processing steps, mass spectrometry based measurements, and data processing steps were performed. The intact protein quantitation method features extraction and integration of m/z data from each charge state of a detected alpha-synuclein species and fitting of the data to a simple linear model which accounts for concentration and charge state variability. The quantitation method was validated with serial dilutions of intact protein standards. Using the method on the human brain samples, several previously unreported modifications in alpha-synuclein were identified. Low levels of phosphorylated alpha synuclein were detected in brain tissue fractions enriched for Lewy body pathology and were marginally significant between PD cases and controls (p = 0.03).

P arkinson's disease (PD) is a progressive neurodegenerative disorder. It is a proteinopathy in which alpha-synuclein has been implicated to play a key role in pathogenesis and pathophysiology[1–3]. Alpha-synuclein is a 140 amino acid protein that misaggregates in the disease tissue and forms a major constituent of the hallmark pathology of Parkinson's disease termed Lewy bodies[4–6]. A number of post-translational modifications (PTMs) of alpha-synuclein, such as phosphorylation, truncation, and nitration have been reported in PD brain tissue[7–9]. Some of these modifications, specifically phosphorylation of Ser129 and C-terminal truncations at residues 119–121, for example, are thought to accelerate misaggregation of alpha synuclein in *in vitro* tests[10–12]. However, comprehensive and unbiased assessment of the abundance of different modified alpha-synuclein proteoforms in brain tissue has not been performed. Such studies are needed to gain insights into pathogenic forms of alpha-synuclein.

The analysis of intact proteins by mass spectrometry (MS) was identified as a promising use of electrospray ionization (ESI) technology shortly after the advent of ESI[13–14]. However, despite the early ESI work performed on both peptides and proteins, the ease-of-use for protein identification by digestion-based methods gave peptide-based proteomics considerable advantages over intact protein analyses. Today, almost all MS-based proteomics quantitation work is performed using sophisticated methods to infer original protein levels after digestion and analysis at the peptide level. However, with the emergence of high-throughput intact protein characterization by MS, there is an opportunity for further development of intact protein quantitation.

Through MS instrument advancement and front-end separation technologies, intact mass determination and fragmentation, the "top-down" method, has become an established tool capable of analyses of mixtures of intact proteins by use of online liquid chromatography (LC)-ESI-MS[15–16]. Different proteins and proteoforms are

readily detected and differentiated, thereby enabling the interrogation of post-translational modifications of proteins. One of the key advantages to the top-down approach is the definitive characterization of each of a protein's proteoforms, a crucial step in deciphering a protein's ultimate function or potential disease role.

Various methods of MS-based quantitation of peptides are used to determine protein expression and abundance for targeted and systems-based research[17–20]. Recently, advances in mass spectrometer hardware and data processing software have enabled sophisticated peptide quantitation[21–23]. The nature of intact protein ESI is such that charge follows a predictable Gaussian distribution over many states at different m/z. Quantification of complex protein MS data has been limited to picking the most intense peak or summing all charge state signals together - with little supporting evidence for processing rationale beyond a single protein of interest[24–28]. The objective of the present set of studies was to develop a method for intact protein quantitation by ESI-MS to quantify alpha-synuclein proteoforms from control and Parkinson's disease tissues.

A simple but powerful method for intact protein assessment by ESI-MS and quantitation of the abundance via serial dilutions of standard proteins is reported here. Automated peak integration software (not required, but helpful) and statistical modeling approaches to aggregate data across charge states were applied to provide accurate, relative abundance of intact and modified alpha-synuclein protein forms. The frontal cortex of clinically and pathologically characterized normal controls, PD and PD cases with co-occurring Alzheimer's disease were assessed. The data provide evidence of several hitherto unreported truncations of alpha-synuclein and the presence of alpha-synuclein phosphorylated at serine 129 in pathology-enriched and disease tissue, thereby demonstrating the utility of the method.

Results

LC-MS for Serial Dilutions of Intact Protein Standards. Data for 16 two-fold serial dilutions of alpha-synuclein (starting at 100 ng on column) and ubiquitin (starting at 50 ng on column) in standard protein matrix were plotted with area under the curve (AUC) from all charge states detected as a function of protein amount on column (Supplementary Figure 1). The observations from Supplementary Figure 1 are as expected: as total protein amount on column decreases, lesser-abundant charge states are not detected. Supplementary Figure 2 shows exemplary alpha-synuclein LC-MS data from protein standards and from immunoprecipitated brain lysate tissue. Such data convey the typical S/N ratios observed and slight degree of artificial oxidation observed.

A model was constructed using data from each dilution for all charge states of a given protein at the unoxidized state. The results of this model for the two dilution series are shown in Figure 1. Data are modeled based on the approach similar to that proposed by Higgs et al. shown below[29].

$$log_{10}(AUC_{ij}) = \mu + Z_j + S_j + \varepsilon_{ij} \qquad (1)$$

In Eq. 1, AUC_{ij} is the observed charge state peak area for the ith charge state of the jth sample. Z_i represents the charge state term and is attributed to the ith charge state which reflects abundances for each charge state. S_j represents the sample term and is attributed to the jth sample which reflects what the model aims to estimate: varying levels of the protein in different samples. μ represents the overall mean (intercept), and ε_{ij} is the residual error $\sim N(0,\sigma^2)$. This additive model on log-transformed peak areas is motivated from the assumption that electrospray XIC peak areas are proportional to the product of a charge state specific constant (Z) and sample concentration (S) of the protein ($AUC_{ij} \sim Z_iS_j$). This log-linear relationship follows naturally from the observation that ESI-MS peak areas are proportional to the product of two terms: protein concentration and a charge state

factor[14]. Peak areas that are discordant with this linear model are candidates for exclusion (or down weighting) when estimating overall relative protein abundance in the samples. Discordance could arise from an interfering peak corrupting specific charge states in some samples by either ion suppression or co-elution and contamination of integrated peak areas. Discordance of charge state peak areas is addressed by analyzing the residuals from the regression described in Eq. 1 using standard M-estimation and iteratively weighted least squares via the robust linear modeling function "rlm" in the MASS package of R[30].

From Figure 1, the model values for serial dilutions in a standard protein matrix more closely trend with the theoretical dilution (grey line) than either the sum or the mean. Coefficients of variation estimated for ^{15}N alpha-synuclein, ubiquitin, and lysozyme were 7.6%, 10.1%, and 16.8%, respectively for the alpha-synuclein dilution. Coefficients of variation estimated for alpha synuclein and lysozyme were 4.7% and 10.0%, respectively for the ubiquitin dilution. Coefficients of variance are presented to demonstrate repeatability of measurement. Overall from Figure 1, an advantage in lower limit of quantification is gained from using the model compared to summing or averaging, particularly in the case of alpha-synuclein.

The deviation in the mean from model derived charge states for the alpha-synuclein dilution series in a standard protein matrix is shown in Supplementary Figure 3, indicated by a line plot. Reconstruction of the charge state effect from the model can serve as a check of the data *a posteriori*. Two key features of the modeling approach are that missing charge state peak areas are systematically addressed and that peak areas contaminated by co-eluting species are excluded from XIC integration via the robust linear model fitting. To examine the ability of the modeling to address these situations, data from four ubiquitin dilution samples were modified to simulate noise. The measured peak areas for charge states $7+$, $8+$, and $10+$ in four ubiquitin dilutions were replaced with log_{10} normal (Gaussian) random noise values (mean = 7, st.dev. = 1), and a randomly selected 20% of the remaining peak areas from ubiquitin were removed prior to reanalysis. These data show that robust linear modeling approach was substantially better at reproducing the expected two-fold ratio for the four data-modified samples relative to a non-robust model, the mean of log_{10} transformed peak areas, and the sum of the peak areas (Supplementary Table 1). Here, the robust modeling within R performed as expected for corrupted or otherwise compromised data. Non-robust modeling does not perform well under such conditions. The robust linear modeling approach was used in this study to handle any peak areas that were potentially noise-corrupted.

**Application of Protein Quantitation Model to IP-MS of Alpha-Synuclein from Brain Lysate.** The model in Eq. 1 was applied to MS data with ^{15}N alpha-synuclein spiked into human brain lysate as an internal reference standard prior to IP-LC-MS analysis. Correlation of the model-derived AUC signal between the heavy and endogenous alpha-synuclein is shown in Supplementary Figure 4A. A high variance in detection of endogenous alpha-synuclein (y-axis) is seen on the plot, and the CV is calculated to be 25% before normalization to the heavy standard. After normalization in each sample to the heavy alpha-synuclein signal, the CV is calculated to be 8.3%. In Supplementary Figure 4B, internal standard-normalized, model-derived protein estimates of alpha-synuclein AUCs are shown with scaling set to a maximum of 10^8 and the y-axis range set to two-fold. The sources of variation are separated and displayed along the bottom of the plot to break out individual variance components. The contributions to variance by the day of experiment, tissue lyses, IPs within lysates, and residual (attributed to LC-MS) are shown along with their variance components in Supplementary Table 2. Data show minimal to no variance contributed by the lysis and IP steps.
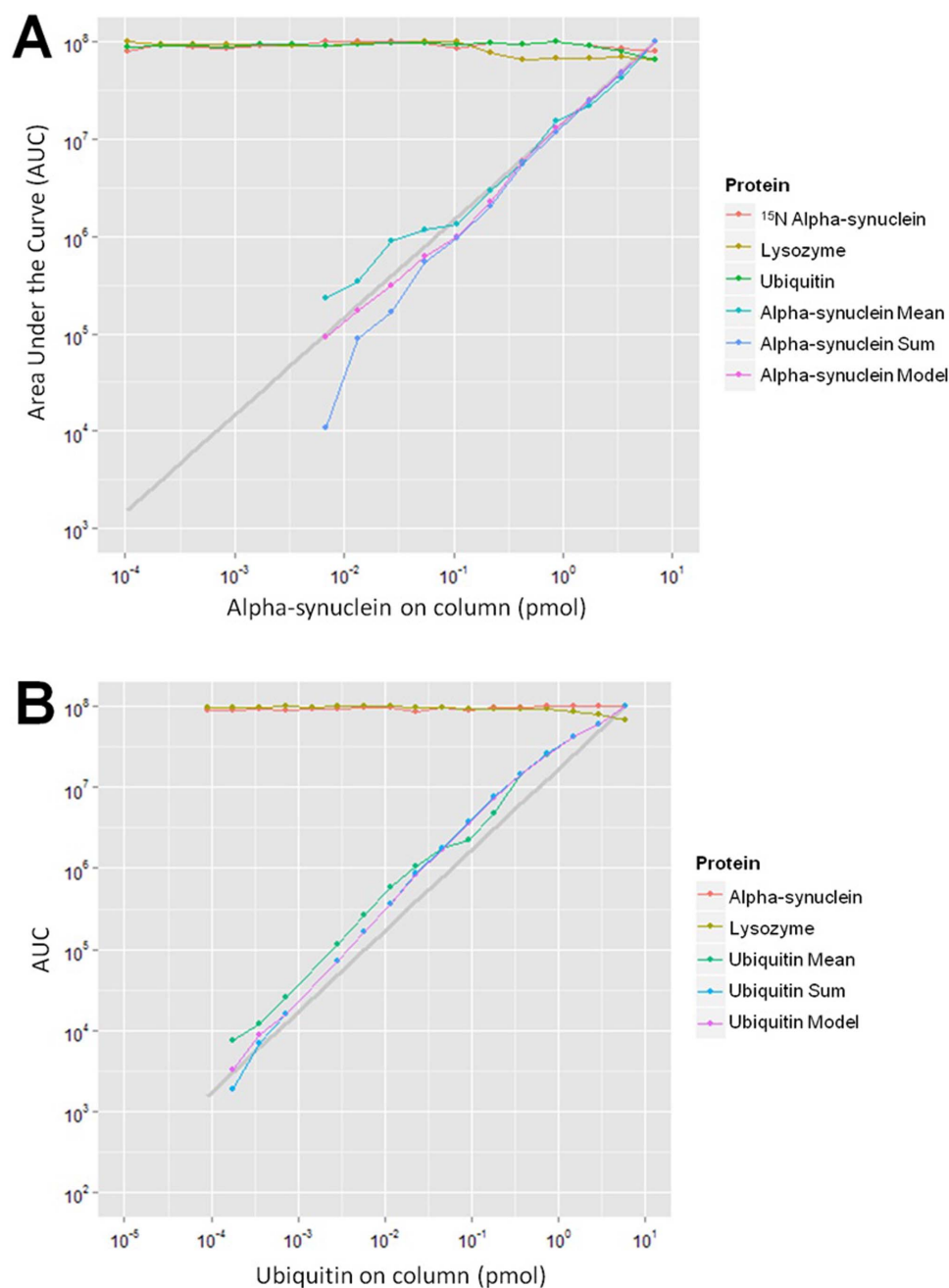
Figure 1 | Serial dilution of alpha synuclein (A) and ubiquitin (B) in standard protein matrix with model derived protein level estimates and mean charge state values. AUCs are maximum-scaled to 10^8. ''Protein mean'' indicates estimates derived by taking the mean of the $\log_{10}$ charge state peak areas. ''Protein sum'' indicates estimates derived by taking the sum of the $\log_{10}$ charge state peak areas. The grey line represents a theoretical linear dilution from the highest point with the intercepts set to zero. The model, mean, and sum plots are presented for comparison to the theoretical dilution. Here, the ''Protein model'' gives a more accurate estimation of protein concentration than either the ''Protein sum'' or ''Protein mean'' quantitation methods, particularly at low protein concentrations.

Data modeling represented in Supplementary Figure 4 was executed by first performing individual protein modeling then normalization based on model estimates. Thus, one approach to take is modeling first and normalizing second. However, another approach to handle experiments with labeled protein present is to normalize the data to the labeled standard before applying the model. In principle, there is no difference between the two approaches; however, in practice there could be small differences caused by missing value patterns between the endogenous and labeled protein robust weighting. Thus, another approach would be to normalize data first and perform modeling second. Charge-state terms of Eq. 1 with modeling

performed after normalization to ^{15}N-labeled alpha-synuclein are shown in Supplementary Figure 5. After normalization, approximately equal ratios for each charge state are shown for the alpha-synuclein standards dilution experiment (from Figure 1A), indicated by a dashed line. Despite normalization prior to modeling for the brain lysate experiment (from Supplementary Figure 4), charge state bias is still present. The presence of charge state bias indicates a non-linear relationship of peak area ratios with respect to charge (solid line). Charge state bias in this case is likely to arise from the MS signal of less-abundant charge states of a less-abundant protein falling below the baseline of chemical noise (matrix background).
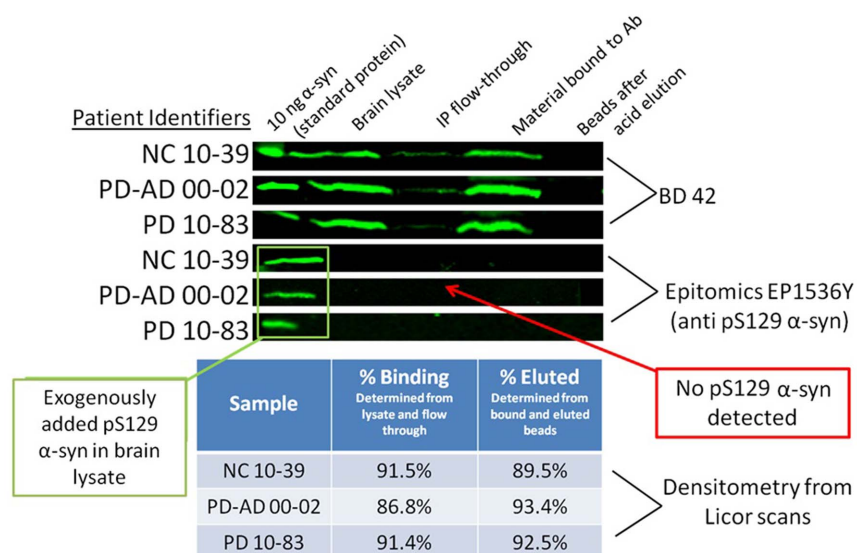
Figure 2 | Evidence for total alpha-synuclein recovery throughout immunoprecipitation and elution steps for the SDS-soluble fraction. Total alpha-synuclein recovery is assessed with the BD42 antibody (top). The percent binding and eluted are calculated from the densitometry to estimate recovery for each step. The Epitomics antibody is used to survey for phosphorylated alpha-synuclein. The pS129 standard is spiked into brain lysate, but no endogenously phosphorylated alpha-synuclein is detected in the SDS-soluble fraction.

The presented intact protein LC-MS quantification method was developed to address a need to quantitate intact alpha-synuclein from human brain tissue. For the patient samples, a sample and staging scores summary is presented Supplementary Table 3. The cohorts include 10 PD cases, 6 cases of PD with Alzheimer's disease, and 16 age-matched, normal controls. Tissue samples were collected within three hours post mortem. The analytical workflow for these samples featured two separate LC-MS injections. The first injection was intact protein mass measurement only for quantification analysis. The second injection was intact protein mass measurement followed by fragmentation for protein characterization. The overall CV of the protocol, as performed for this study (2 cm LC separation column), was observed as 9.2% from normalized, quantitative MS estimates of 12 replicate LC-MS injections from a single IP of control brain tissue.

Evidence for recovery from the IP and elution steps is shown in Figure 2. From three patient samples, material from each step of the protocol was saved for protein recovery assessment by western blot using the BD Clone 42 (total alpha-synuclein) antibody and survey for pS129 alpha-synuclein using an Epitomics anti-pS129 alpha-

synuclein antibody. Depletion of alpha-synuclein during IP binding and elution are presented, and recovery for each of the steps was determined by quantification of total alpha-synuclein before and after IP and elution. From densitometry from LICOR scanning, the recovery is estimated at ~90% for each the binding and elution step for an estimated 80% recovery of total alpha-synuclein. Phosphorylated alpha-synuclein standard was spiked into brain lysate to demonstrate stability and detectability. No endogenous phosphorylated alpha-synuclein was detected in the 37°C SDS-soluble fraction.

Alpha-synuclein characterization results of the analysis of the SDS-soluble fraction of frontal cortex from 32 patient samples are presented in Table 1. The best identification score for each characterized form is presented. All presented forms are definitively characterized from accurate intact and fragment masses with matching fragments in the b- and y- directions and confident P-Values from the statistical scoring in ProSight. Several of the modifications were also confirmed by Glu-C digest analysis. Ten truncated alpha-synuclein forms along with full-length alpha-synuclein were characterized in the SDS-soluble fraction; five truncated forms were

| Table 1	Endogenous, SDS-soluble alpha-synuclein forms characterized by intact protein mass spectrometry			
	Theoretical	Observed	Number of	
Alpha-synuclein Form	Mass (Da)	Delta Mass (ppm)	Matching Fragments	P-Value
71–140*†#	7369.4	0.1	36	1×10^{-42}
68–140*†#	7596.6	1.8	51	2×10^{-64}
66–140#	7752.6	1.0	14	3×10^{-15}
65–140†#	7866.7	1.8	9	3×10^{-11}
Ac 1–101#	10097.4	1.4	44	3×10^{-49}
39–140*#	10593.1	1.1	35	3×10^{-36}
Ac 1–119*	12049.3	2.0	35	2×10^{-39}
Ac 1–122 (deamidation N122)*†	12376.4	3.6	22	6×10^{-25}
Ac 1–135*	13904.0	3.5	20	1×10^{-12}
5–140*#	13959.0	1.6	30	3×10^{-24}
Ac 1–140*†	14493.2	3.9	48	5×10^{-55}

*Form also characterized in SDS-insoluble fraction.
†Site identified additionally by Glu-C digestion data.
#Form previously unreported *in vivo*.
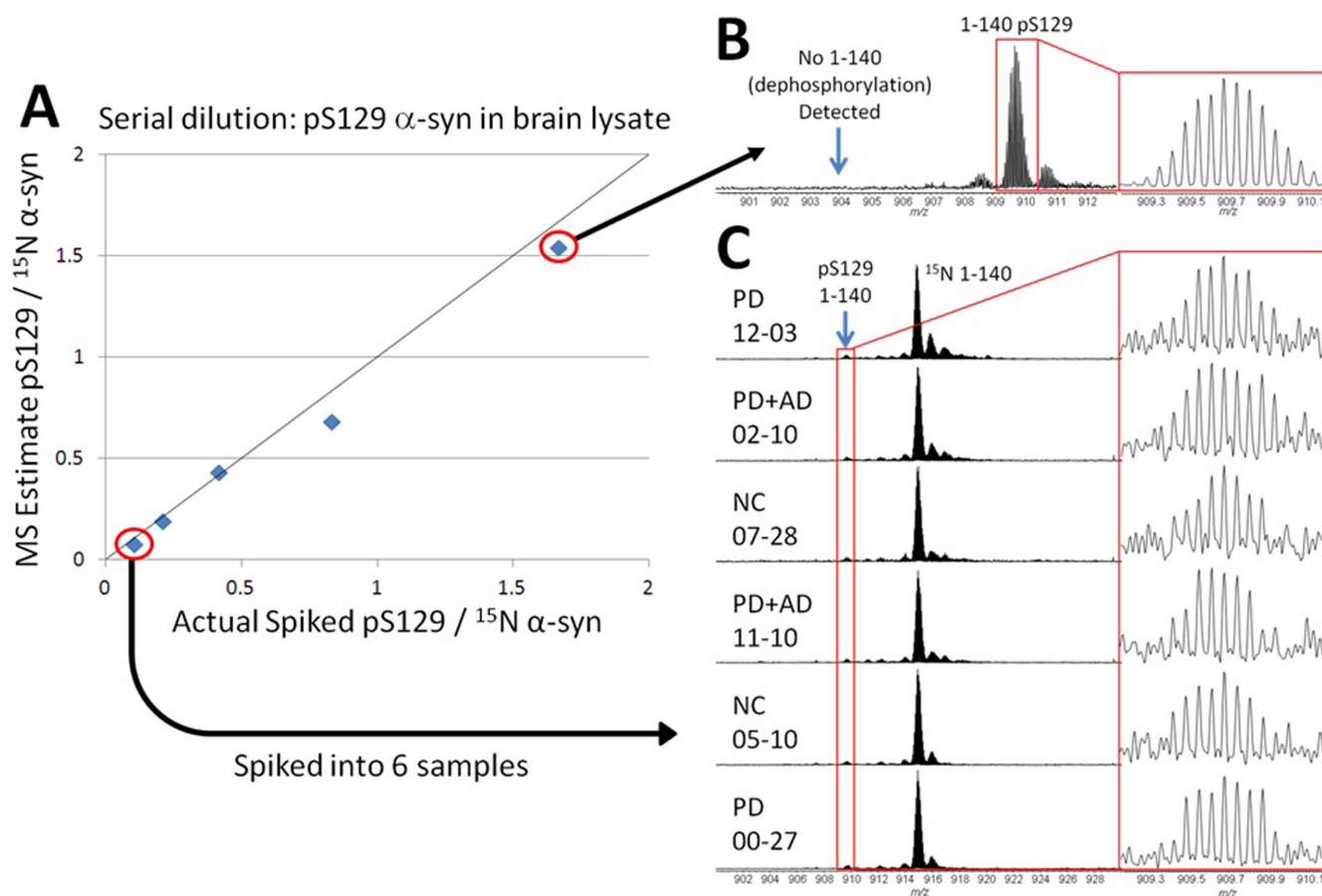
Figure 3 | Recovery of pS129 alpha-synuclein standard and establishment of detection limit. In A, a serial dilution of alpha-synuclein standard in brain lysate is performed. The ^{15}N alpha-synuclein internal reference standard is spiked at a constant amount. The y = x plot is shown to demonstrate linearity, and the MS model estimate of the ratio of pS129 to ^{15}N alpha-synuclein matches well with the actual spiked amount. From the largest spike amount, the pS129 is detected with a high signal-to-noise ratio and no dephosphorylation is observed from the protocol (B). The limit of detection (4 ng of pS129 alpha-synuclein per 1 mg human cortex) is spiked into six patient samples and recovered in each case (C). Endogenously phosphorylated alpha-synuclein was not detected in the SDS-soluble fraction from cortex at the intact protein level or by digestion analyses in these samples.

characterized from the SDS-insoluble fraction along with full-length alpha-synuclein. The exact mass (± 5 ppm) for phosphorylated alpha-synuclein was detected in 7 total samples in the SDS-insoluble fraction, but levels were too low to confirm the site of phosphorylation by MS/MS fragmentation. Also, phosphorylated alpha-synuclein was detected by western blot with an anti-pS129 antibody in several of the same samples (data not shown), thus providing further validation of the MS method.

To establish the limit of detection for pS129 alpha-synuclein from the SDS-soluble fraction, serial dilutions of pS129 alpha-synuclein standard spiked into brain lysate were performed (Figure 3). In 3A, the dilution is plotted with the MS model estimates of the ratio of pS129 alpha-synuclein to ^{15}N alpha-synuclein as a function of the actual ratio of pS129 alpha-synuclein to ^{15}N alpha-synuclein standards spiked into brain lysate ($r^2 = 0.993$). The y = x line is plotted for reference. Data from the largest spike amount is shown to demonstrate pS129 detection with high signal, and evidence for lack of dephosphorylation is presented with no 1–140 alpha-synuclein (unacetylated) present in the run above the limit of detection (3B). The lowest amount on the curve (4 ng of pS129 alpha-synuclein per 1 mg human cortex) is spiked into six patient samples (3C). The pS129 alpha-synuclein is detected in all six samples and established as the limit of detection - approximately 5% relative to full length endogenous alpha-synuclein in the samples shown in 3C.

Quantification results from the reported characterized alpha-synuclein proteoforms are shown in Table 2 and Table 3. Model output values for each form were compared across samples. Forms that were not detected in individual samples were assigned non-zero noise values to aid statistical analysis. In the SDS-soluble fraction, normalization was not used for quantification because there was no correlation between the ^{15}N-labeled internal standard and the endogenous Ac 1–140 form (*i.e.* there was no systematic variance affecting samples), and root-mean-square error was higher in ANOVAs with normalized response (data not shown). However, for the SDS-insoluble fractions, normalization was used for quantification because there was significant correlation between Ac 1–140 and ^{15}N alpha-synuclein. The endogenous full length acetylated 1–140 form is the most abundant species of alpha-synuclein in all disease cases and does not differ significantly between groups. For each control or disease group, signal for every form is normalized to Ac 1–140 signal within samples in order to convey abundance estimates of quantified forms. Note that the values reported are averaged for detection events only. A tally of detection events for each form is shown for each control or disease group.

For the SDS-soluble fraction, the individual ANOVA P-Values are shown for each form. The Ac 1–140, Ac 1–122, and 39–140 forms were correlated between samples, but the other five forms compared were not correlated and are considered independent tests. To correct for multiple hypothesis testing, a Bonferroni corrected P-Value is shown. Also shown is a column indicating whether or not the test was non-parametric. Non-parametric tests were used in cases with few charge state detection events in disease states for a given form.

Table 2 | Endogenous alpha-synuclein forms from the SDS-soluble fraction of human frontal gyrus quantified by intact protein mass spectrometry

Alpha-synuclein Form	NC Normalized Abundance*	NC Samples with Detection Event	PD Normalized Abundance*	PD Samples with Detection Event	PD + AD Normalized Abundance*	PD + AD Samples with Detection Event	Unadjusted ANOVA P-Value	Bonferroni Corrected P-Value	Test Non-Parametric?
71–140	0.04 ± 0.02	5/16	0.07	1/10	0.02	1/6	0.1	0.5	Yes
68–140	0.03 ± 0.02	11/16	0.01 ± 0.02	4/10	0.03 ± 0.01	2/6	0.1	0.5	Yes
66–140	0.12 ± 0.16	4/16	0.07	1/10	0.06	1/6	N/A†	N/A†	N/A†
65–140	0.14	1/16	0.32	1/10	0	0/6	N/A†	N/A†	N/A†
Ac 1–101	0.13 ± 0.06	2/16	0	0/10	0	0/6	N/A†	N/A†	N/A†
39–140	0.18 ± 0.04	13/16	0.16 ± 0.05	10/10	0.15 ± 0.03	6/6	0.37	1	No
1–119	0.29 ± 0.16	12/16	0.19 ± 0.05	10/10	0.26 ± 0.20	4/6	0.21	1	No
Ac 1–122 (deamidation N122)	0.24 ± 0.05	13/16	0.21 ± 0.07	10/10	0.21 ± 0.05	6/6	0.4	1	No
Ac 1–135	0.21 ± 0.04	16/16	0.17 ± 0.02	10/10	0.19 ± 0.03	6/6	0.81	1	No
5–140	0.45 ± 0.05	11/16	0.31 ± 0.40	2/10	0.04 ± 0.02	2/6	0.013	0.65	Yes
Ac 1–140	1	16/16	1	10/10	1	6/6	0.37	1	No

*Averaged for detection events only and normalized to Ac 1–140 response
†Not enough detection events for valid statistical comparison
NC, Normal Control; PD, Parkinson's Disease; PD + AD, Parkinson's Disease with Alzheimer's Disease

Table 3 | Endogenous alpha-synuclein forms from the SDS-insoluble fraction of human frontal gyrus quantified by intact protein mass spectrometry

Alpha-synuclein Form	NC Normalized Abundance*	NC Samples with Detection Event	PD Normalized Abundance*	PD Samples with Detection Event	PD + AD Normalized Abundance*	PD + AD Samples with Detection Event	Unadjusted P-Value	ANOVA or Chi-Squared Test?
68–140	0.11 ± 0.04	2/16	0.05	1/10	0	0/6	N/A†	N/A†
1–119	0.26 ± 0.10	14/16	0.26 ± 0.08	9/10	0.27 ± 0.06	5/6	0.85	ANOVA
Ac 1–122 (deamidation N122)	0.24 ± 0.09	15/16	0.23 ± 0.07	10/10	0.24 ± 0.07	5/6	0.85	ANOVA
Ac 1–135	0.25 ± 0.09	15/16	0.25 ± 0.08	10/10	0.25 ± 0.08	5/6	0.85	ANOVA
5–140	0.36 ± 0.13	6/16	0.20 ± 0.21	2/10	0.45	1/6	0.49	Chi-Squared
Ac 1–140 (phosphorylated)	0.21	1/16	0.19 ± 0.03	5/10	0.18	1/6	0.03	Chi-Squared
Ac 1–140	1	16/16	1	10/10	1	6/6	0.72	ANOVA

*Averaged for detection events only and normalized to Ac 1–140 response.
†Not enough detection events for valid statistical comparison.

The only form with levels that may be different for the SDS-soluble fraction from cortex in these samples is 5–140, although statistical significance was not reached.

For the SDS-insoluble fraction, the ANOVA or chi-squared P-Values are shown for each form. Here, the Ac 1–140, Ac 1–135, Ac 1–122, and Ac 1–119 were correlated between samples. Neither the 5–140 form nor the mass corresponding to phosphorylated alpha-synuclein were correlated, and the masses were subjected to a chi-squared test for association with a disease state due to a very low number of total observations for those particular proteoforms across normal and disease states. The phosphorylated mass was found in 6 PD and 1 normal sample, and the unadjusted P-Value from the chi-squared test is 0.03. Other characterized masses did not have sufficient detection events to warrant testing.

Discussion

The model estimates from the proteins held at constant amount throughout the dilutions shown in Figure 1 yield CV values which indicate repeatability in measurement for intact protein standards measured by the LC-MS platform presented. A potential concern is behavior of multiple proteins with varying chemistries for quantitation from complex mixtures. For example, co-eluting proteins in a complex mixture may have different ionization efficiencies compared to a low-background or singly-eluted recombinant proteins. For targeted approaches, simple dilution experiments are feasible to determine linear behavior of a single protein; however, inevitably some intact protein quantitation experiments will rely on the assumption of linear relationship to determine fold-change in expression. Although modeling is implemented to account for charge state and ionization effects, the simple proof-of-principle examples presented here may yet require investigators to perform further due-diligence for specific research projects.

Characterization results for 11 alpha-synuclein proteoforms are reported in Table 1. Alpha-synuclein has been characterized by intact protein MS previously[31]. However, in that study, only endogenous full length alpha-synuclein and a single truncation form were reported with data that would provide statistical confidence. Here, several of the truncated forms were also confirmed from Glu-C protease digestion of IP reactions directly on the beads. However, not all truncation forms are identified by digestion, highlighting a key advantage of using the intact protein MS approach.

Truncations of alpha-synuclein in vivo and in aggregation studies have been demonstrated, and several of the truncations reported here are mentioned in previous literature. The 71–140 form was used as a substrate for fibrillogenesis and showed no fibril assembly after 96 hours[32]. The 5–140 form was reported as a minor aggregation product that was increased after an alpha-synuclein protein standard incubation in $FeCl_3$[33]. The 1–135 from has been reported in vivo in Lewy bodies[34]. The 1–119 and 1–122 forms have been reported in vivo and in several aggregation studies[9,11,35,36]. Importantly, we identified several previously unreported N- and C-terminal truncations (see Table 1). The role of these proteoforms in alpha-synuclein aggregation is yet to be established.

Phosphorylated alpha-synuclein is believed to play a role in the pathogenesis of PD, and evidence has been shown for alpha-synuclein pS129 increase with progression of Lewy body pathology in human brain tissue[8,37]. Several steps were taken to validate the method for detection of pS129 alpha-synuclein. The limit of detection pS129 alpha-synuclein, its quantitative and reproducible recovery from brain lysates, and lack of dephosphorylation during sample preparations were established by analysis of serial dilutions of pS129 alpha-synuclein standard spiked into the SDS-soluble fractions. At the limit of detection on the curve (4 ng of pS129 alpha-synuclein per 1 mg brain tissue), pS129 standard was consistently recovered. From the six patient samples tested, the limit of detection for pS129 alpha-synuclein is 5% relative to endogenous full length protein.

Importantly, it is demonstrated that no dephosphorylation occurs during the sample preparation and manipulations within the limit of detection. Also, the serial dilution is linear in brain lysate (r^2 = 0.993). Here, pS129 alpha-synuclein is observed only in the SDS-insoluble, Lewy body enriched fraction. If phosphorylated alpha-synuclein is present in the SDS-soluble fraction it is present at levels below 5% relative to endogenous alpha-synuclein. However, several alpha-synuclein truncation forms were higher than the 5% threshold relative to endogenous alpha-synuclein established for phosphorylated alpha-synuclein in the SDS-soluble fractions in these samples. Hence, the data presented here indicate that neither does pS129 alpha-synuclein exist in high amounts as SDS-soluble monomers or oligomers, nor does it exist consistently in high amounts in the SDS-insoluble fraction of diseased samples.

Quantification results are presented in Table 2 and Table 3. Values normalized to Ac 1–140 are presented to convey protein abundance, but un-normalized protein estimates from the model were used to compare protein levels across samples and conduct statistical analyses. There were a substantial number of missing values, so some non-parametric tests were used. In this study, the levels of 1–119 and 1–122 are not different between control and disease samples in the SDS-soluble fraction of the cortex. In previous work, Li et al. (2005) reported total C-terminal truncations (including 1–119 and 1–122) to have significantly different levels in control vs. disease tissue from SDS-soluble fractions[9]. Possible explanations for the difference between current results and those reported by Li et al. (2005) is heterogeneity in pathology in patient populations or the method of analysis. Li and coworkers compared four cases with the same number of controls; in the present study alpha-synuclein was analyzed in a total of 32 brains leading to better statistical confidence. The phosphorylated alpha-synuclein was rarely detected in this study; there were only 7 total detection events (6 cases and 1 control brain lysate), leading to a marginally significant unadjusted chi-squared P-value of 0.03.

In summary, to the best of the authors' knowledge, this is the first report of a mass spectrometry based quantitative assessment of post-translationally modified alpha-synuclein in a relatively large number of pathologically diagnosed Parkinson's disease and neurological control tissues. The top-down MS identified several reported alpha-synuclein proteoforms as well as previously unreported truncations. Comparison of neurological controls versus disease cases did not identify a disease-segregating truncation; thereby suggesting that truncation of alpha-synuclein in SDS-soluble tissue is a normal process and not an indicator of disease pathology or progression. Furthermore, despite the many PTMs reported for alpha-synuclein, modified alpha-synuclein either exists at levels an order of magnitude lower than some of the truncations, exists as forms not amenable to the immunoprecipitation performed, or exists as high molecular weight species (such as polyubiquitination). The quantitation methods presented are directly applicable for labeled or label free analysis of simple protein mixtures. Note that the linear model based summarization used here to robustly estimate relative protein concentrations in samples is completely analogous to standard approaches used in microarray transcript profiling to summarize how probe sets are summarized to estimate gene levels and to how probesets and exons are modeled to estimate gene levels in the new high density transcript arrays[38,39]. The intact protein quantification modeling could also extend to individual isotopes within a given charge state, and isotope effects could be represented with another term in the formula for the model. Evaluation of quantitation at the isotope level would be necessary and could greatly eliminate the chance for error if different proteins to be quantified have overlapping isotope distributions. With further studies, the methods could be expanded to quantitation for top-down proteomics studies, opening a new realm for proteomics research.
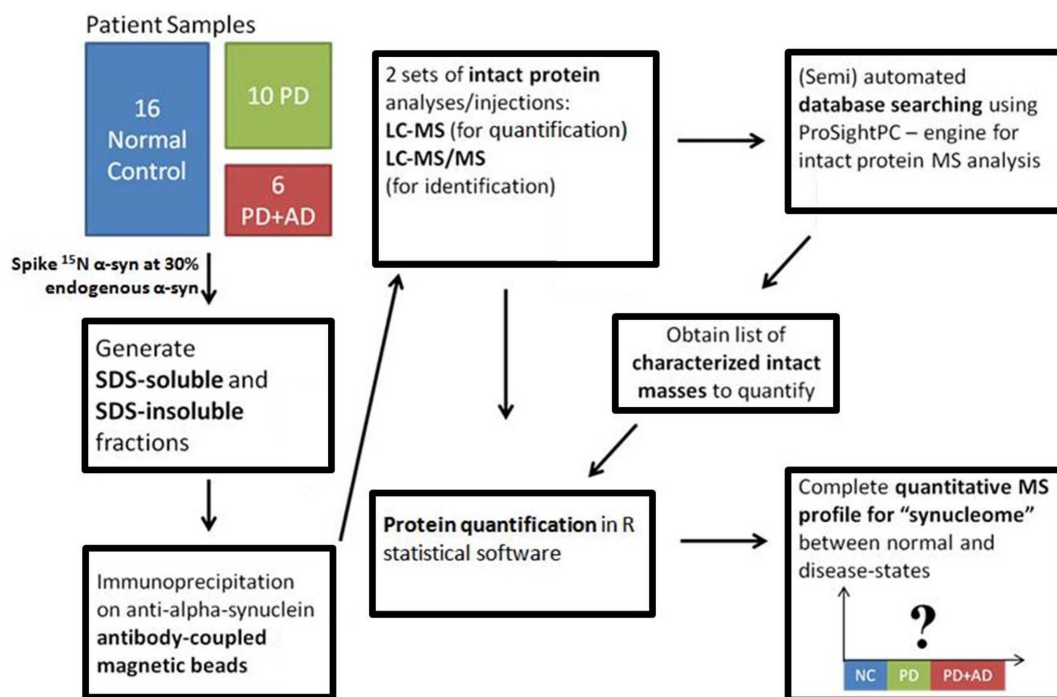
Figure 4 | Schematic of sample analysis workflow.

Methods

Standard Protein Preparation. The following protein standards were purchased from Sigma-Aldrich (St. Louis, MO): ubiquitin (U6253), lysozyme (L7651), and carbonic anhydrase (C2624). Proteins were resuspended in water to 2 g/L, aliquoted, and frozen at -80°C for one-time use. The following standards were purchased from rPeptide (Bogart, GA): alpha-synuclein (S-1001-1) and ^{15}N-labeled alpha-synuclein (S-1004-1). The ^{15}N-labeled alpha-synuclein serves as a stable isotope label for normalization. Commercial alpha-synuclein proteins were resuspended in water to 2 g/L, frozen at -80°C and aliquoted for one-time use. Phosphorylated alpha-synuclein at S129 was prepared in-house using polo-like kinase 2[40].

Standard Protein Mixture Preparation. Ubiquitin dilutions were prepared by diluting the 2 g/L stock to 50 ng/µL in 0.1% formic acid (Thermo Fisher Scientific). The sample was diluted in 0.1% formic acid for 16 successive two-fold dilutions down to 0.00076 ng/µL at the lowest ubiquitin injection. The proteins alpha-synuclein and lysozyme were prepared at a concentration of 10 ng/µL in 0.1% formic acid to be held constant in each ubiquitin dilution sample. For each 5 µL LC-MS injection, 1 µL of ubiquitin dilution, 1 µL alpha-synuclein and lysozyme mix, and 3 µL 0.1% formic acid were combined.

Alpha-synuclein dilutions were prepared by diluting the 2 g/L stock to 100 ng/µL in 0.1% formic acid. The sample was diluted in 0.1% formic acid for 16 two-fold dilutions down to 0.0015 ng/µL at the lowest alpha-synuclein injection. The proteins lysozyme, ubiquitin, carbonic anhydrase, and ^{15}N-labeled alpha-synuclein were prepared in a mix in 0.1% formic acid to be held constant in each alpha-synuclein dilution sample. Lysozyme was prepared at a concentration of 10 ng/µL, ubiquitin was prepared at 2 ng/µL, carbonic anhydrase was prepared at 8 ng/µL, and ^{15}N alpha-synuclein was prepared at 30 ng/µL. For each 5 µL injection, alpha-synuclein dilution (1 µL), lysozyme, ubiquitin, carbonic anhydrase, and ^{15}N-labeled alpha-synuclein mix (1 µL), and 3 µL 0.1% formic acid were combined.

Intact Protein Standard LC-MS Data Acquisition. For validation using standard protein dilutions in a standard protein matrix, samples were injected onto 10 cm × 75 µm BIOBASIC C4 pulled-tip analytical picofrit column (New Objective, Woburn, MA). Samples were loaded and separated using an Easy nLC II nanoflow LC system (Thermo Fisher Scientific, San Jose, CA) at a flow rate of 1 µL/min. The gradient flowed at a rate of 300 nL/min and increased from 2% LC buffer B (0.1% formic acid in acetonitrile) to 20% B in 5 minutes, 50% B in 25 minutes, 80%B in 6 minutes, and decreased to 2% B in 9 minutes. Samples were analyzed using an LTQ Orbitrap Velos (Thermo Fisher Scientific). Intact protein MS data were detected with four microscans at a resolution setting of 60,000 with an in-source fragmentation setting of 15 volts to energetically remove non-covalent adducts.

Specimen Collection and Preparation. For method validation, a 1 g specimen of frontal cortex from normal human brain tissue (Analytical Biological Services Inc., Wilmington, DE), collected 5 hours post-mortem from a 90 year-old female, was triturated on a bed of dry ice to give 20–50 mg pieces. The weights of frozen pieces were recorded. Five pieces were individually lysed on one day and six pieces were

individually lysed on another day for a total of 11 brain lyses. There were two IP reactions per lysate and two LC-MS injections per IP reaction for a total of 44 LC-MS injections.

For study analysis, frontal gyrus was collected from 32 volunteer research subjects who died and were autopsied as part of the Banner Sun Health Research Institute Brain and Body Donation Program[41]. All enrolled subjects or legal representatives signed an Institutional Review Board-approved informed consent form[41]. The complete workflow for patient samples from beginning to end is shown in Figure 4. The mean post-mortem interval prior to tissue collection was approximately 3 hours for all groups (see Supplementary Table 3). Consensus criteria were used to diagnose AD and PD in these cases, and to distinguish PD from dementia with Lewy bodies. The brains of all subjects were scored and staged for alpha-synucleinopathy load and distribution according to the Unified Staging System for Lewy Body Disorders. A 1 g specimen was triturated on a bed of dry ice to give 20–50 mg pieces. The weights of frozen pieces were recorded.

Briefly, anti-alpha synuclein antibody was coupled to magnetic beads, and an immunoprecipitation reaction was performed on solubilized tissue fractions. Alpha-synuclein was eluted using glacial acetic acid (Proteochem, Cheyenne, WY) and diluted two-fold with 0.1% formic acid (Thermo Fisher Scientific, San Jose, CA) for analysis by LC-MS.

Antibody Coupling to Magnetic Beads. Borate buffer was prepared as follows: 3 g of boric acid (Sigma), 20 mL of water, 5 mL of a 5 N NaOH (Sigma) solution were combined. The mixture was diluted to a final volume of 50 mL for a concentration of 1 M borate. The final pH of this buffer was 9.5. Dynabeads MyOne Tosylactivated (Invitrogen, Carlsbad, CA) were resuspended and 333 µL were transferred to a clean tube. Using a magnet, the supernatant was collected then discarded. Beads were rinsed with 0.1 M borate buffer pH 9.5. Using a magnet, the supernatant was collected then discarded. Then, 400 µg of purified Clone 42 anti-alpha-synuclein antibody (BD Biosciences, San Jose, CA) was added to the beads along with 100 µL of 1 M borate buffer pH 9.5. The mixture was diluted to a final volume of 1 mL. The beads were incubated by rotating overnight at room temperature. After the overnight incubation, 50 µL of 1 M Tris-HCl pH 8.0 (Invitrogen) were added for an additional one hour at room temperature with gentle rotation. Using a magnet, the supernatant was collected then discarded, and the beads were washed with 1 mL phosphate-buffered saline (PBS, Invitrogen) buffer three times. Beads were resuspended in 1 mL PBS and stored at 4°C.

Bead Washing for SDS-Insoluble IP Reactions. Because of lower amounts of endogenous alpha-synuclein present in the SDS-insoluble fraction, there was a need for enhanced signal in the MS and it was found that additional washes of antibody-coupled beads enhanced recovery. Thus, beads used for SDS-insoluble IP reactions required additional washes. After the Tris-HCl wash described above, beads were washed additionally in RIPA buffer for 96 hours. Using a magnet, the RIPA supernatant was collected then discarded, and the beads were washed with 1 mL phosphate-buffered saline (PBS, Invitrogen) buffer three times. Beads were resuspended in 1 mL PBS and stored at 4°C.

Sample Preparation and IP Conditions. Single pieces of brain tissue (25–50 mg) were homogenized in lysate buffer at a ratio of 2 µL buffer per 1 mg of tissue. Lysate buffer contained 750 mM NaCl (Sigma), 20 mM Tris-HCl buffer, pH 7.5 (Invitrogen), 5 mM EDTA (Invitrogen), 0.1% SDS (Invitrogen), 5 mM methionine (Sigma), protease and phosphatase inhibitor (#88669, Thermo Fisher Scientific), and ^{15}N-labeled alpha-synuclein at 1 µg per 50 µL of lysate buffer. After homogenization, samples were heated to 55°C for 5 minutes. Sonication buffer was then added at a ratio of 10 µL buffer per 1 mg of tissue. Sonication buffer contained 1% triton X-100 (Sigma), 50 mM Tris-HCl buffer, pH 8.0, 200 mM NaCl, 5 mM methionine, and protease and phosphatase inhibitor (#88669, Thermo Fisher Scientific). Samples were sonicated on ice three times for ten seconds each. After sonication, samples were centrifuged at 15,000 RPM for 30 minutes at 4°C. Supernatants were transferred into clean tubes. For each IP, 36 µL of supernatant was used. The 36 µL of supernatant corresponds roughly to 3 mg of brain tissue based on volumes used in the lysis and sonication procedures. To each sample IP, 750 µL of RIPA buffer was added. RIPA buffer consisted of 200 mM NaCl, 0.6% deoxycholic acid (Sigma), 0.6% nonidet P40 (American Bioanalytical, Inc., Natick, MA), 20 mM Tris, pH 8.0, 5 mM methionine, and protease and phosphatase inhibitor (#88669, Thermo Fisher Scientific). Finally, 10 µL of anti-alpha-synuclein magnetic beads were added per tube and incubated at 4°C overnight with shaking.

Additional Sample Preparation for SDS-Insoluble Fraction. First, 20 µL lysate buffer for each 50 mg wet brain weight was added to a washed pellet centrifuged at 25,000 × g at 4°C for 30 minutes from the aforementioned protocol for separation of SDS-soluble and SDS-insoluble fractions. For spike experiments, a separate lysis was performed for insoluble material. For insoluble material, 1 mg/ml ^{15}N alpha-synuclein was diluted 100 fold in water and spiked at 0.02 µL of diluted standard per each 1 mg starting material (1 µL diluted standard per pellet from 50 mg starting wet brain weight). Samples were sonicated on ice three times at ten seconds each. Then, samples were heated to 99.5°C in a heating block for 15 minutes. After cooling to room temperature, 100 µL IP dilution buffer was added per 50 mg wet brain weight. Samples were sonicated on ice three times at ten seconds each. Samples were then centrifuged at 15,000 RPM at 4°C for 30 minutes. Supernatant was saved for IP reaction. For IP reaction, 500 µL RIPA buffer was added to sample along with 25 µL beads washed for SDS-insoluble IP reactions. Samples were incubated overnight with shaking.

IP Washing and Elution Conditions. Using a magnet, the supernatant from the immunoprecipitation was collected then discarded. Beads were washed as follows: 1 mL RIPA buffer (one time), 1 mL PBS (one time), 1 mL water (one time). For SDS-soluble IP reactions, proteins were eluted from the beads with 5 µL glacial acetic acid twice. For SDS-insoluble IP reactions, proteins were eluted from the beads with 6 µL glacial acetic acid once. Prior to LC-MS injection, samples were diluted two-fold with 0.1% formic acid (LC Buffer A).

Intact Protein LC-MS Data Acquisition from Human Samples. For study samples, samples were injected onto 2 cm × 150 µm BIOBASIC C4 fritted column (New Objective, Woburn, MA). Samples were eluted to an empty Picofrit column (New Objective). Samples were loaded and separated using an Agilent LC system with Nano Flow controller (Santa Clara, CA). Five µL of each sample (20 µL total) were loaded at a flow rate of 1 µL/min in 98% LC Buffer A (0.1% formic acid) and 2% LC Buffer B (0.1% formic acid in acetonitrile, Thermo Fisher Scientific) for 15 minutes and directed to waste. The flow was decreased from 1 µL/min to 0.5 µL/min over 5 minutes, and the gradient was increased to 30% LC Buffer B over the same 5 minutes. Flow was then directed to the spray tip. The gradient increased to 60% LC Buffer B over 29 minutes, then to 80% LC Buffer B in 5 minutes. The flow was then directed back to waste. Flow was increased to 1 µL/min over 1 minute. Flow was held at 80% LC Buffer B for two minutes. The gradient was then decreased to 2% LC Buffer B over 9 minutes and held constant for 5 minutes until the end of the run. Samples were analyzed using an LTQ Orbitrap Velos (Thermo Fisher Scientific). MS data were detected with four microscans at a resolution setting of 60,000 with an in-source fragmentation setting of 15 volts. MS/MS data were collected with a top 2 data dependent acquisition mode at the 30,000 resolution setting with CID settings as follows: isolation width of 10 m/z, collision energy of 35 volts, activation time of 100 ms, and activation Q of 0.4. The top eight charge state peaks for full length acetylated alpha-synuclein and ^{15}N alpha-synuclein internal reference standard were placed on a global exclusion list. MS and MS/MS were performed in separate LC-MS injections.

MS/MS Data Processing. Protein characterization was performed by use of ProSightPC 2.0 (Thermo Fisher Scientific). An alpha-synuclein database annotated with known PTMs and mutations was created within the ProSightPC software using the database manager in the software, and MS data was searched within ProSightPC against this database. Data was searched using "absolute mass" mode (searches for exact masses of intact species) and "biomarker" mode (searches for non-enzymatic cleavages and proteolysis). All characterized proteins reported were manually validated and included exact masses for intact and fragment ions as well as fragment ions matched in both the b- and y- directions.

Western Blot Analysis. For western blot analysis, 5% of each sample from steps in the protocol was saved for SDS-PAGE. To each sample, 1 µL of BlueJuice loading buffer (Invitrogen, Carlsbad, CA) was added, and the sample was diluted to 10 µL. Samples

were run on 4–20% tris-glycine SDS-PAGE gel (Invitrogen), 30 mA (constant) for 1.5 hr. Gels were transferred to a 0.2 µm nitrocellulose membrane (Biorad, Hercules, CA) at 500 mA (constant) for 1 hr. using A Criterion Blotter (Biorad). Blots were fixed with 0.4% paraformaldehyde (Sigma-Aldrich, St. Louis, MO) in PBS (Invitrogen) for 30 minutes to fix the protein to the membrane. Membranes were processed using the BenchPro 4100 Card Processing Station (Invitrogen) for western blot analysis. The system was operated according to manufacturer instructions. The blots were placed in SEA BLOCK blocking buffer (Thermo) for 120 minutes. Blots were washed in PBS with 2% Tween 20 (Sigma) for 1 minute. Blots were incubated in primary antibody (Clone 42, BD Biosciences, Franklin Lakes, NJ or EP1536Y, Epitomics, Burlingame, CA) in 2% Tween 20 for 600 minutes. Blots were then washed in PBS with 2% Tween 20 for 20 minutes, followed by incubation in IRDye 800 CW Goat anti-Mouse or anti-Rabbit IgG antibody (Licor, Lincoln, NE) for 60 minutes. Blots were then washed again in PBS with 2% Tween 20 for 20 minutes and then held in SEA BLOCK blocking buffer. Blots were imaged using a Licor Odyssey Imaging System per manufacturer instructions.

Glu-C Digestion Analysis - Bottom-Up Reversed-Phase LC-MS/MS. A second immunoprecipitation reaction was performed from 3 mg of remaining lysate from the preparations described above. However, instead of eluting washed IPs, the washed IPs were saved for digestion analysis. One-half of the total bead volume was combined with 10 µL 1 M Tris HCl pH 8.0 (Invitrogen) with 1 µg of Glu-C (Roche, Indianapolis, IN) added. Samples were digested at room temperature overnight. Peptides were extracted and purified by use of a µC18 ZipTip (Millipore, Billerica, MA). ZipTips were equilibrated with 50% acetonitrile in 0.1% trifluoroacetic acid (Thermo) followed by 0.1% trifluoroacetic acid. Samples were passed through the tip, and the tip was washed ten times with 0.1% trifluoroacetic acid. Peptides were eluted with 1.5 µL of 50% acetonitrile in 0.1% trifluoroacetic acid. Samples were diluted to 10 µL in LC buffer A. Five µL of diluted peptides were injected onto a 7 cm × 75 µm YMC-gel C18 pulled-tip analytical picofrit column (New Objective). Samples were loaded and separated using an Easy nLC II nanoflow LC system (Thermo Fisher Scientific). Samples were loaded at a flow rate of 1 µL/min. The gradient flowed at the rate of 300 nL/min and increased from 2% LC buffer B to 40% buffer B in 30 minutes, then increased to 90% B in 10 minutes. Samples were run on an Orbitrap Elite (Thermo) using high-resolution (30,000 resolution setting) for the intact scan and a top 12, data dependent acquisition for fragmentation detection at low resolution in the ion trap. Data acquisition and analysis for peptide identification was performed as previously described[29].

Data processing for protein quantitation. Thermo LC-MS files were processed in an automated fashion using in-house software but the steps are simple enough to be replicated with programming knowledge or even manual processing. The steps of the software are outlined in Supplementary Scheme 1. An LC-MS file was opened in the software, and values from the *.raw data file were used to deconvolute charge state peaks using a custom algorithm All spectra were displayed in the mass domain. Mass domain isotope peaks can be fit to theoretical isotope distributions for monoisotopic mass detection based on an averagine table. Once a mass was detected, in-house software enabled selection of an extracted ion chromatogram (XIC) from the most intense charge (displayed in a separate window) for the detected protein mass of interest. The time range corresponding to the elution of the protein mass was selected by the user. XICs were then generated based on the detected mass of interest. For each potential protein charge state, the isotope distribution must yield a detection of the mass of interest for a charge state XIC to be generated. As a result, XICs from all detected charge states from the protein mass of interest in the time range were generated. To determine the width of the XIC in the m/z domain, the m/z range was set to include the top 66% of the theoretical isotope peaks. The software reported areas in the selected time range for all detected charge states. Alternatively, the data from each mass can be extracted manually in Xcalibur (Thermo) software for each charge state at each m/z to yield the same information acquired from automated processing.

All modeling analyses were conducted using the mass package in R[30]. Implementation of the proposed modeling approach is straightforward in the R language: 'fitted.model <- rlm(logauc ~ Sample + Zstate, data = mydata, method = "M")' can be executed on a data frame called 'mydata' containing the log transformed peak areas for each charge state in each sample.

Statistical Comparisons. All comparisons for quantified alpha-synuclein were performed in JMP 9.0 (SAS, Cary, NC). Traditional one-way ANOVA tests were performed where applicable. For alpha-synuclein proteoforms with substantial missing values, a chi-squared test was used to test for the association between detected/not detected and the disease group. To determine if changes were significant, model values from un-normalized protein peak areas across samples were used for statistical comparisons.

1. Gong, C.-X., Liu, F., Grundke-Iqbal, I. & Iqbal, K. Post-translational modifications of tau protein in Alzheimer's disease. *J. Neural Transm.* **112**, 813–838 (2005).
2. Wang, Y., Lin, F. & Qin, Z.-H. The role of post-translational modifications of huntingtin in the pathogenesis of Huntington's disease. *Neurosci. Bull.* **26**, 153–162 (2010).
3. Oueslati, A., Fournier, M. & Lashuel, H. A. Role of post-translational modifications in modulating the structure, function and toxicity of α-synuclein:

Implications for Parkinson's disease pathogenesis and therapies. *Prog. Brain Res.* **183**, 115–145 (2010).

4. Spillantini, M. G. *et al.* α-Synuclein in Lewy bodies. *Nature* **388**, 839–840 (1997).

5. Baba, M. *et al.* Aggregation of alpha-synuclein in Lewy bodies of sporadic Parkinson's disease and dementia with Lewy bodies. *Am. J. Clin. Pathol.* **152**, 879 (1998).

6. Hurtig, H. *et al.* Alpha-synuclein cortical Lewy bodies correlate with dementia in Parkinson's disease. *Neurology* **54**, 1916–1921 (2000).

7. Oueslati, A., Paleologou, K. E., Schneider, B. L., Aebischer, P. & Lashuel, H. A. Mimicking Phosphorylation at Serine 87 Inhibits the Aggregation of Human α-Synuclein and Protects against Its Toxicity in a Rat Model of Parkinson's Disease. *J. Neurosci.* **32**, 1536–1544 (2012).

8. Walker, D. G. *et al.* Changes in Properties of Serine 129 Phosphorylated α-Synuclein with Progression of Lewy-type Histopathology in Human Brains. *Exp. Neurol.* (2013).

9. Li, W. *et al.* Aggregation promoting C-terminal truncation of α-synuclein is a normal cellular process and is enhanced by the familial Parkinson's disease-linked mutations. *Proc. Natl. Acad. Sci. U.S.A* **102**, 2162–2167 (2005).

10. Conway, K. A., Rochet, J.-C., Bieganski, R. M. & Lansbury, P. T. Kinetic stabilization of the α-synuclein protofibril by a dopamine-α-synuclein adduct. *Science* **294**, 1346–1349 (2001).

11. Greenbaum, E. A. *et al.* The E46K mutation in α-synuclein increases amyloid fibril formation. *J. Biol. Chem.* **280**, 7800–7807 (2005).

12. Takahashi, T., Yamashita, H., Nakamura, T., Nagano, Y. & Nakamura, S. Tyrosine 125 of α-synuclein plays a critical role for dimerization following nitrative stress. *Brain Res.* **938**, 73–80 (2002).

13. Fenn, J. B., Mann, M., Meng, C. K., Wong, S. F. & Whitehouse, C. M. Electrospray ionization for mass spectrometry of large biomolecules. *Science* **246**, 64–71 (1989).

14. Smith, R. D., Loo, J. A., Edmonds, C. G., Barinaga, C. J. & Udseth, H. R. New developments in biochemical mass spectrometry: electrospray ionization. *Anal. Chem.* **62**, 882–899 (1990).

15. Ouvry-Patat, S. A. *et al.* Top-down proteomics on a high-field Fourier transform ion cyclotron resonance mass spectrometer. *Methods Mol. Biol.* **492**, 215–231 (2009).

16. Kellie, J. F. *et al.* The emerging process of Top Down mass spectrometry for protein analysis: biomarkers, protein-therapeutics, and achieving high throughput. *Mol. Biosyst.* **6**, 1532–1539 (2010).

17. Oda, Y., Huang, K., Cross, F., Cowburn, D. & Chait, B. Accurate quantitation of protein expression and site-specific phosphorylation. *Proc. Natl. Acad. Sci. U.S.A.* **96**, 6591–6596 (1999).

18. Old, W. M. *et al.* Comparison of label-free methods for quantifying human proteins by shotgun proteomics. *Mol. Cell. Proteomics* **4**, 1487–1502 (2005).

19. Ong, S. E. *et al.* Stable isotope labeling by amino acids in cell culture, SILAC, as a simple and accurate approach to expression proteomics. *Mol. Cell. Proteomics* **1**, 376–386 (2002).

20. Ross, P. L. *et al.* Multiplexed protein quantitation in Saccharomyces cerevisiae using amine-reactive isobaric tagging reagents. *Mol. Cell. Proteomics* **3**, 1154–1169 (2004).

21. MacLean, B. *et al.* Skyline: an open source document editor for creating and analyzing targeted proteomics experiments. *Bioinformatics* **26**, 966–968 (2010).

22. Reiter, L. *et al.* Aebersold, R: mProphet: automated data processing and statistical validation for large-scale SRM experiments. *Nat. Methods* **8**, 430–435 (2011).

23. Gillet, L. C. *et al.* Targeted data extraction of the MS/MS spectra generated by data-independent acquisition: a new concept for consistent and accurate proteome analysis. *Mol. Cell. Proteomics* **11**, O111.016717 (2012).

24. Oran, P. E. *et al.* Mass spectrometric immunoassay of intact insulin and related variants for population proteomics studies. *Proteomics Clin. Appl.* **5**, 545–459 (2011).

25. Hess, C. *et al.* Simultaneous determination and validated quantification of human insulin and its synthetic analogues in human blood serum by immunoaffinity purification and liquid chromatography-mass spectrometry. *Anal. Bioanal. Chem.* **404**, 1813–1822 (2012).

26. Ruan, Q., Ji, Q. C., Arnold, M. E., Humphreys, W. G. & Zhu, M. Strategy and its implications of protein bioanalysis utilizing high-resolution mass spectrometric detection of intact protein. *Anal. Chem.* **83**, 8937–8944 (2011).

27. Collier, T. S., Sarkar, P., Rao, B. & Muddiman, D. C. Quantitative top-down proteomics of SILAC labeled human embryonic stem cells. *J. Am. Soc. Mass Spectrom.* **21**, 879–889 (2010).

28. Waanders, L. F., Hanke, S. & Mann, M. Top-down quantitation and characterization of SILAC-labeled proteins. *J. Am. Soc. Mass Spectrom.* **18**, 2058–2064 (2007).

29. Higgs, R. E., Butler, J. P., Han, B. & Knierman, M. D. Quantitative proteomics via high resolution MS quantification: capabilities and limitations. *Int. J. Proteomics* **2013**, 1–10 (2013).

30. R Core Team: *A Language and Environment for Statistical Computing.* R Foundation for Statistical Computing, Vienna, Austria (2013).

31. Öhrfelt, A. *et al.* Identification of novel α-synuclein isoforms in human brain tissue by using an online nanoLC-ESI-FTICR-MS method. *Neurochem. Res.* **36**, 2029–2042 (2011).

32. Zibaee, S. *et al.* Sequence determinants for amyloid fibrillogenesis of human α-synuclein. *J. Mol. Biol.* **374**, 454–464 (2007).

33. Vlad, C., Iurascu, M. I., Slamnoiu, S., Hengerer, B. & Przybylski, M. in Intrinsically Disordered Protein Analysis 399–412 (Springer, 2012).

34. Anderson, J. P. *et al.* Phosphorylation of Ser-129 is the dominant pathological modification of α-synuclein in familial and sporadic Lewy body disease. *J. Biol. Chem.* **281**, 29739–29752 (2006).

35. Liu, C.-W. *et al.* A Precipitating Role for Truncated α-Synuclein and the Proteasome in α-Synuclein Aggregation: Implications for Pathogenesis of Parkinson Disease. *J. of Biol. Chem.* **280**, 22670–22678 (2005).

36. Mishizen-Eberz, A. J. *et al.* Cleavage of α-synuclein by calpain: potential role in degradation of fibrillized and nitrated species of α-synuclein. *Biochemistry* **44**, 7818–7829 (2005).

37. Lue, L. F. *et al.* Biochemical Increase in Phosphorylated Alpha-Synuclein Precedes Histopathology of Lewy-Type Synucleinopathies. *Brain Pathol.* **22**, 745–756 (2012).

38. Irizarry, R. A. *et al.* Exploration, normalization, and summaries of high density oligonucleotide array probe level data. *Biostatistics* **4**, 249–264 (2003).

39. McCall, M. N., Jaffee, H. A. & Irizarry, R. A. fRMA ST: frozen robust multiarray analysis for Affymetrix Exon and Gene ST arrays. *Bioinformatics* **28**, 3153–3154 (2012).

40. Inglis, K. J. *et al.* Polo-like kinase 2 (PLK2) phosphorylates α-synuclein at serine 129 in central nervous system. *J. Biol. Chem.* **284**, 2598–2602 (2009).

41. Beach, T. G *et al*, The Sun Health Research Institute Brain Donation Program: description and experience, 1987-2007. *Cell Tissue Bank* **9**, 229–245 (2008).

Acknowledgments

Author contributions

J.K. conducted experiments, wrote the main manuscript text, and prepared all figures. R.H. Did the stastical analysis, J.R. conducted experiments, A.M. developed software, T.B. and C.A. provided tissue, K.M. reviewed the manuscript and M.K. designed experiments and reviewed the manuscript.

Additional information